



An Investigation of the Steady-State Performance of a Pivoted Shoe Journal Bearing with ISO VG 32 and VG 68 Oils

KEITH BROCKWELL (Fellow, STLE; Deceased) and WALDEMAR DMOCHOWSKI (Member, STLE)

National Research Council
Institute for Aerospace Research
Ottawa, Ontario, Canada
and

SCAN DECAMILLO (Member, STLE)
Kingsbury, Inc.
Philadelphia, Pennsylvania

This article presents a report on an investigation into the performance characteristics of a steadily loaded pivoted shoe journal (PSJ) bearing that is lubricated with ISO VG 32 and VG 68 oils. The article describes a testing machine on which the experimental investigation was performed. Measurements of shaft torque, pad temperature distributions, oil inlet and outlet temperatures, oil flow rate, and eccentricity have all been recorded as functions of load and speed. The experimental results from both test oils are presented in graphical form and are compared with theoretical predictions obtained from the author's computer model of the PSJ bearing. These results showed that the thicker ISO VG 68 oil provided thicker oil films. However, it also had higher bearing temperatures and power losses. A good correlation between the theoretical and experimental results has been found. Theoretical analysis of the bearing friction losses indicate that shear losses predominate and churning losses account for approximately 20% of the total losses.

KEY WORDS

Bearings; Hydrodynamic; Fluid Film; Tilting Pad

INTRODUCTION

When it comes to lubricating pivoted shoe journal (PSJ) bearings, the lubricant grade is typically based on the application. Low-speed/high-load applications often use ISO VG 68 oil to maintain a thicker oil film, whereas the majority of high-speed/low-load applications use light turbine oil, ISO VG 32, to keep pad temperatures and power losses at manageable levels. In between, there are cases where lubricant grade benefits overlap. There are also reasons to consider a change from the recommended lubricant, which may

be the case in an upgrade or when different applications (e.g., a gearbox and compressor) share a common lube system. In such situations, the changes in bearing performance need to be assessed.

A number of authors have presented steady-state results from experimental work on PSJ bearings. This includes studies of bearing and bulk oil temperatures, over a wide range of bearing sizes, speeds, and unit loads (Brockwell, et al. (1), (2); Simmons and Dixon (3); Simmons and Lawrence (4); DeChoudhury and Masters (5); DeChoudhury and Barth (6)). Others have measured shaft-to-bearing displacements, also over a wide range of operating conditions (Brockwell and Kleinbub (7); Pettinato and DeChoudhury (8); Tripp and Murphy (9)). All of the studies mentioned are based on tests using light turbine oils.

The purpose of this article is to fill a gap in the literature by providing information from PSJ bearing tests comparing bearing performance using ISO VG 32 and ISO VG 68 oils. Shaft torque, bearing and bulk oil temperatures, and shaft displacements have been recorded for various loads and speeds. Comparisons are made between the experimental results and theoretical predictions.

TEST RIG

A schematic of the test apparatus is shown in Fig. 1. It consists of a test bearing, the shaft and drive system, the loading system, and the rig supporting structure.

A full description of the test rig is given in the literature (Brockwell, et al. (1)). Briefly, it consists of a 152.4-mm-diameter shaft, driven by a 112-kW variable speed DC electric motor. Using a belt and pulley system, a maximum shaft speed of just over 16,000 rpm is attained. The shaft is supported on two 0.09-m-diameter tilting-pad journal bearings, spaced about 0.7 m apart. A slotted optical switch in conjunction with a shaft-mounted disk with a number of drilled holes measures shaft speed.

The rig features a pneumatic system that applies load to the test bearing through two hydrostatic bearings shown in Fig. 2. The lower hydrostatic bearing provides the test bearing with lateral freedom. The upper spherical hydrostatic bearing allows

Presented at the ASME/STLE Tribology Conference
In Cancun, Mexico
October 27-30, 2002
Final manuscript approved May 9, 2004
Review led by Alan Palazzolo

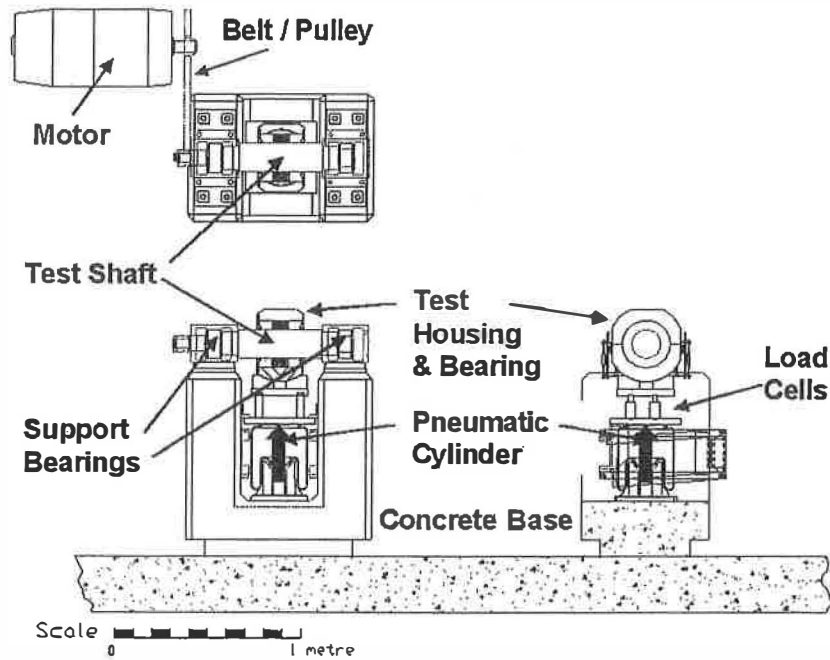


Fig. 1—Schematic of bearing test rig.

the bearing housing to be used as a low-friction torque-sensing device. This provides a more precise determination of bearing power loss than the thermal balance method. A balance arm, in conjunction with a load cell, is used to record the friction torque directly.

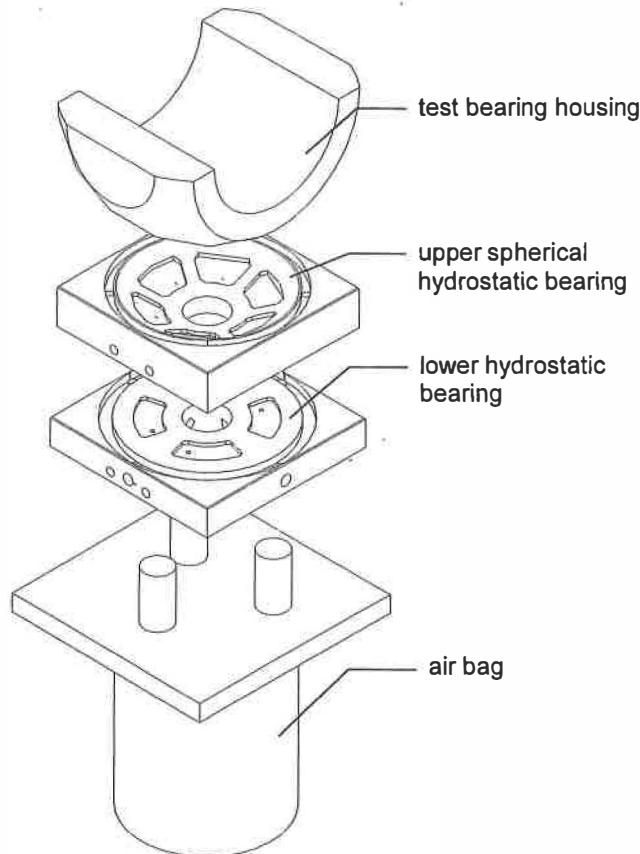


Fig. 2—Loading system.

Proximity probes arranged in two mutually perpendicular axes at either end of the bearing housing measure shaft eccentricity. These probes measure the horizontal and vertical displacements of the test bearing with respect to the shaft's location. They also provide a check of the alignment between the bearing and shaft. Signals from probes mounted directly opposite each other were combined to give the true relative position because this setup canceled out any shaft bending effects. Measurements from both ends of the bearing housing were then averaged to determine the displacements (in both orthogonal planes) at the midplane of the bearing. Steady-state eccentricities were measured with respect to an equilibrium position, which was determined at 72 m/s with zero load on the bearing after thermal equilibrium had been established in the bearing.

A pump with a capacity of $1.26 \times 10^{-3} \text{ m}^3/\text{s}$ and a maximum supply pressure of 2.1 MPa delivers oil to the test bearing from a 0.6 m³ capacity tank. The flow rate is measured by a turbine-type flow meter with a linear flow range of 0.16×10^{-3} to $1.83 \times 10^{-3} \text{ m}^3/\text{s}$. Feed oil temperature is measured as it enters the test bearing and is controlled by a water-oil heat exchanger to within $\pm 1^\circ\text{C}$. An industrial-type pressure transducer, with a 0 to 0.41 MPa operating range, measures the oil supply pressure to the test bearing. Thermocouples monitor the oil inlet temperature and the oil outlet temperature from each side of the test bearing.

Measurement uncertainties are listed in Table 1.

TEST BEARINGS

The test bearing had a nominal diameter of 152 mm and a pad axial length of 67 mm. The assembled bearing diametral clearance was 0.23 mm, and the nominal pad preload was 0.25. The pads had a 60° included angle and a pivot offset of 60%. Pads are steel backed with a babbitt surface.

TABLE 1—MEASUREMENT UNCERTAINTIES

Measurement	Type of Sensor	Limit of Error of Sensor
Temperature	Type-T thermocouple	1°C or 0.75% (whichever is greater)
Shaft speed	Optical switch	±5 rpm
Bearing load	0-10 kN load cells (×3)	±25 N at full scale
Oil flow rate	Turbine flow meter	±0.5% of reading
Oil supply pressure	Pressure transducer	±0.02 MPa
Shaft displacement	Eddy current probe	±0.5% of reading

Pad pivots were of rolling contact design, with two different radii of curvature in the circumferential and axial directions. The circumferential curvature permits each pad to change its tilt to accommodate changing operating conditions. The axial curvature allows the pads to align themselves to the shaft.

Lubricant was fed to the bearing through five radial holes that direct oil from an annulus on the outside of the bearing carrier ring to the spaces between the pads. Drainage of oil from the bearing occurred by way of a small annular clearance between the bearing end plates and the shaft. This setup ensures that the bearing cavity always runs full of oil and at a slight positive pressure. Details are shown in Fig. 3.

The test bearings were instrumented with an array of 45 type-T thermocouples with the tip of each thermocouple located 0.5 mm below the babbitt's surface. The loaded pads were more heavily instrumented along the centerline and included additional thermocouples sited along the edges of the pads. Figure 4 provides details on the locations as a percentage of the pad arc length.

TEST CONDITIONS

- Tests were performed over a range of speeds and loads.
- Applied bearing loads were 3.51, 14, and 22.24 kN (0.34, 1.38, and 2.19 MPa unit loads).
- Oil flow rates used in the tests are listed in Table 2.
- Tests were performed with the "load between pads."
- Table 3 lists the oil properties of the ISO VG 32 and VG 68 turbine oils.
- Oil supply temperature was 49°C.

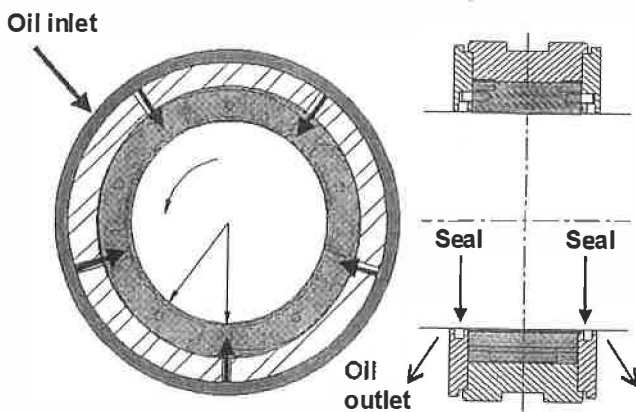


Fig. 3—Flood-lubricated PSJ bearing.

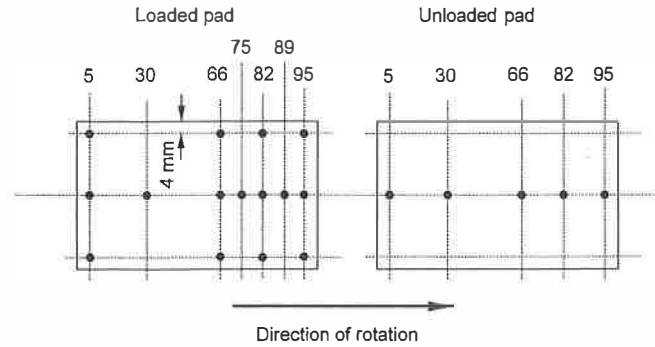


Fig. 4—Thermocouple locations—test bearing.

COMPUTER MODEL

The author's computer model of the PSJ bearing has been described in detail elsewhere (Dmochowski (10)). Briefly, the pressure distribution in the oil film is calculated from a two-dimensional version of the Reynolds equation. This considers viscosity variations in the circumferential and radial directions and assumes the Swift-Steiber boundary condition for a cavitated oil film. Film turbulence is included in the model.

The temperature distribution in the oil film is governed by the energy equation. This accounts for heat conduction across the oil film and heat convection in the circumferential direction. The energy equation is solved assuming the following boundary conditions: 1) that the shaft temperature is equal to the average of all the pad temperature distributions, 2) that there is a certain temperature distribution at the pad surface (calculated from the heat transfer equation), and 3) that the pad leading-edge temperature is constant through the thickness of the oil film. The third boundary condition is calculated on the basis that hot oil from the preceding pad affects the oil temperature at the leading edge of the next pad.

TABLE 2—TEST OIL FLOW RATES

Load, kN (lb)	Speed, rpm	Flow rate, m ³ /s (US gpm)
3.51 (788)	1,800	5.7 × 10 ⁻⁵ (0.9)
	3,600	1.4 × 10 ⁻⁴ (2.2)
	5,810	2.9 × 10 ⁻⁴ (4.6)
	7,750	4.8 × 10 ⁻⁴ (7.5)
	9,040	6.5 × 10 ⁻⁴ (10.2)
14 (3150)	10,650	9.1 × 10 ⁻⁴ (14.4)
	1,800	7.3 × 10 ⁻⁵ (1.15)
	3,600	1.7 × 10 ⁻⁴ (2.7)
	5,810	3.4 × 10 ⁻⁴ (5.4)
	7,750	4.9 × 10 ⁻⁴ (8.5)
22.24 (5000)	9,040	7.2 × 10 ⁻⁴ (11.3)
	10,650	9.9 × 10 ⁻⁴ (15.6)
	1,800	8.2 × 10 ⁻⁵ (1.3)
	3,600	1.9 × 10 ⁻⁴ (3)
	5,810	3.7 × 10 ⁻⁴ (5.8)
	7,750	5.7 × 10 ⁻⁴ (9)
	9,040	7.5 × 10 ⁻⁴ (11.8)
	10,650	1 × 10 ⁻³ (16.2)

TABLE 3—LUBRICANT VISCOSITY AND DENSITY INFORMATION

	Viscosity @ 40°C, m ² /s (cSt)	Viscosity @ 100°C, m ² /s (cSt)	Density, g/ml
ISO VG 32 oil	32.76 × 10 ⁻⁶ (32.76)	5.41 × 10 ⁻⁶ (5.41)	0.87 @ 15°C
ISO VG 68 oil	69.88 × 10 ⁻⁶ (69.88)	8.89 × 10 ⁻⁶ (8.89)	0.88 @ 20°C

Temperature distribution at the pad surface is calculated from the Laplace heat transfer equation, assuming a constant temperature in the axial direction. The boundary conditions for the heat transfer equation correspond to an equality of heat fluxes at the boundary between the oil film and the pad surface, and heat convection on all remaining surfaces.

Approximate pad deflection is calculated from the one-dimensional equation for a beam. Shear forces, bending moments, and local differences in temperature across the thickness of the pad are taken into consideration. In the axial direction, the load distribution is assumed constant and is calculated by averaging the pressures in this direction. Boundary conditions at the pivot correspond to zero surface deflection and zero gradient.

By simultaneously solving these equations for each individual pad, the solution for the entire bearing is obtained.

The computer model accounts for three sources of power loss. The first is the viscous shear in the oil film between the surface of the journal and the surfaces of the loaded and unloaded pads, including film turbulence. The second is commonly referred to as churning loss. This is attributed to losses in the spaces between the pads as a result of the oil being exposed to the journal's moving surface. The third is the kinetic loss, which occurs as a result of accelerating the oil in the bearing up to the speed of the shaft. Appendix A shows how the second and third losses are determined.

DISCUSSION OF RESULTS

In this study, measurements of shaft torque, pad temperature distributions, oil inlet and outlet temperatures, oil flow rate, and eccentricity have all been recorded as functions of load and speed. Performance comparisons for the two oil grades are based on identical operating conditions of load, speed, oil flow, and oil inlet temperature. In addition, the experimental results from both test oils are compared with theoretical predictions obtained from the author's computer model of the PSJ bearing.

Shaft Torque

The upper spherical hydrostatic bearing allowed the bearing housing to be used as a low-friction torque-sensing device. Used in conjunction with a balance arm and a load cell, the torque on the shaft was measured directly and then used to calculate the bearing's power loss.

Figure 5 shows the relationship between bearing power loss and shaft speed for the ISO VG 32 oil. Although power loss varies with load and speed, it can be seen that speed has a far greater effect on power loss. For example, with a unit load of 2.19 MPa, the power loss of the bearing is virtually tripled as a result of raising the shaft speed from 46 to 85 m/s. On the other hand, at

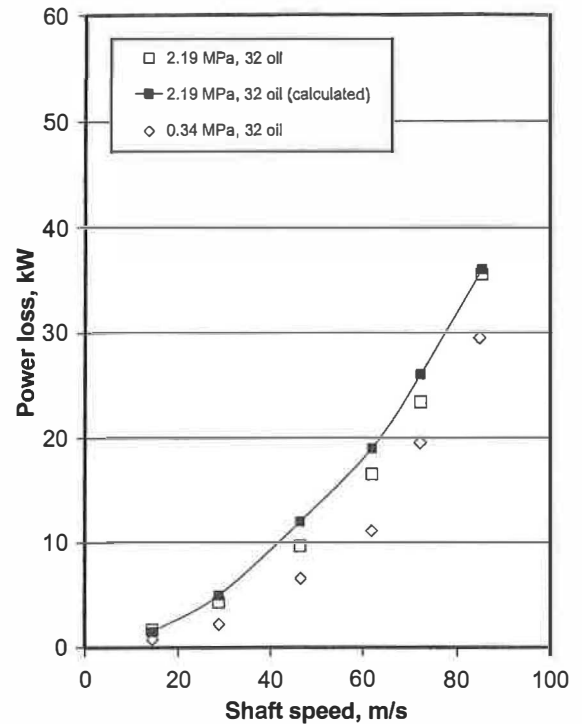


Fig. 5—Variation in power loss with shaft speed—ISO VG 32 oil.

85 m/s shaft speed there is only an approximate 20% increase in power loss as a result of increasing the unit load from 0.34 to 2.19 MPa. There is good correlation between the experimental and calculated power losses for the 2.19 MPa unit load condition. Figure 6 shows the significance of the various losses calculated by the theoretical model. Over the range of test speeds, shear losses predominate and account for over 90% of the total losses at low

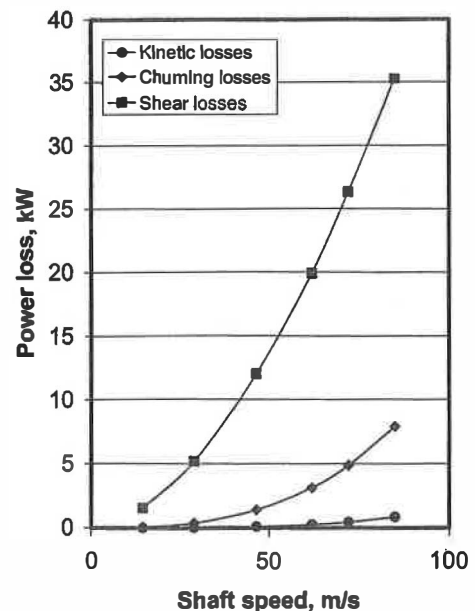


Fig. 6—Calculated distribution of power losses in a PSJ bearing—ISO VG 32 oil.

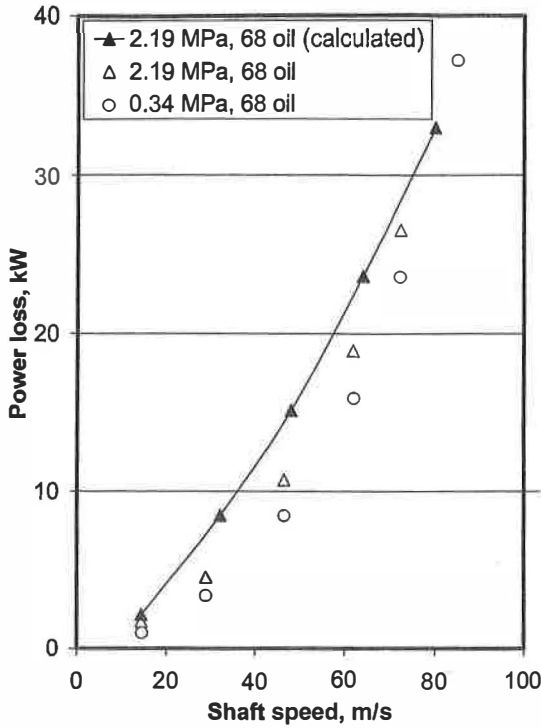


Fig. 7—Variation in power loss with shaft speed—ISO VG 68 oil.

speeds and between 80 and 90% at higher speeds. Churning losses make up most of the balance, with the kinetic losses accounting for only 1–2% of the total losses.

Figure 7 shows the relationship between bearing power loss and shaft speed for the ISO VG 68 oil. With this thicker oil, losses are larger than those recorded with the ISO VG 32 oil, but not significantly so. For example, with a shaft speed of 72 m/s and a unit load of 2.19 MPa, the measured losses with the ISO VG 32 and 68 oils were 23 and 27 kW, respectively. This smaller-than-expected difference is attributed to much higher pad temperatures encountered using ISO VG 68 oil (compared in the next section). The higher temperatures significantly lower the oil film viscosity and, therefore, the shear losses within the bearing, which account for 80–90% of the total losses.

Bearing Temperatures

Both the loaded and unloaded pads were heavily instrumented with thermocouples, as shown in Fig. 4. Particular attention was paid to the trailing half of the two loaded pads, since it is within these regions of the bearing that the maximum operating temperature occurs. Also, on both loaded pads, thermocouples were installed at the 75% location, a location used in many industrial specifications (e.g., API Standard 670 (11)). There are several benefits in using a heavy array of thermocouples. It allows for a more accurate depiction of pad temperature profiles and provides a means to determine the maximum temperature and location on the pad surface. The side detectors are checked to assure there is no significant misalignment that would add gross errors to comparisons.

The second loaded pad in the direction of rotation ran hottest and the maximum temperature was close to the trail-

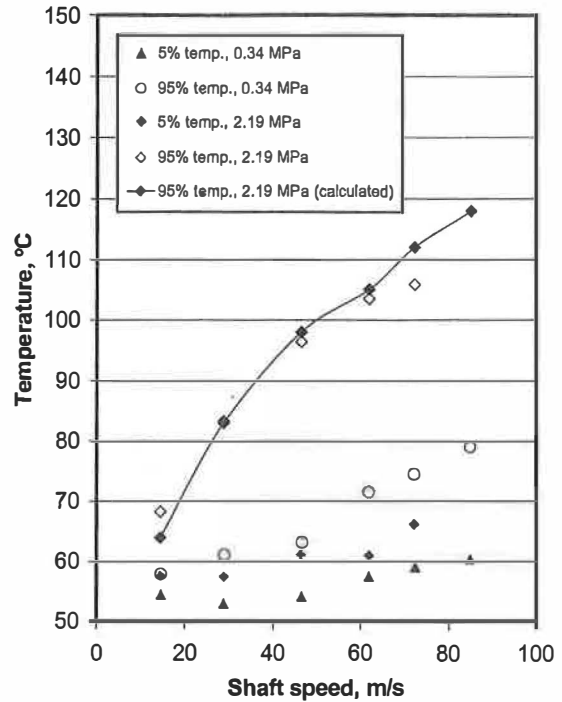


Fig. 8—Effect of shaft speed on second loaded pad temperatures—ISO VG 32 oil.

ing edge for both oils and for all operating conditions tested. Figures 8 and 9 show the effect of shaft speed on the second loaded pad leading- (5% location) and trailing- (95% location) edge temperatures for the ISO VG 32 and 68 oils,

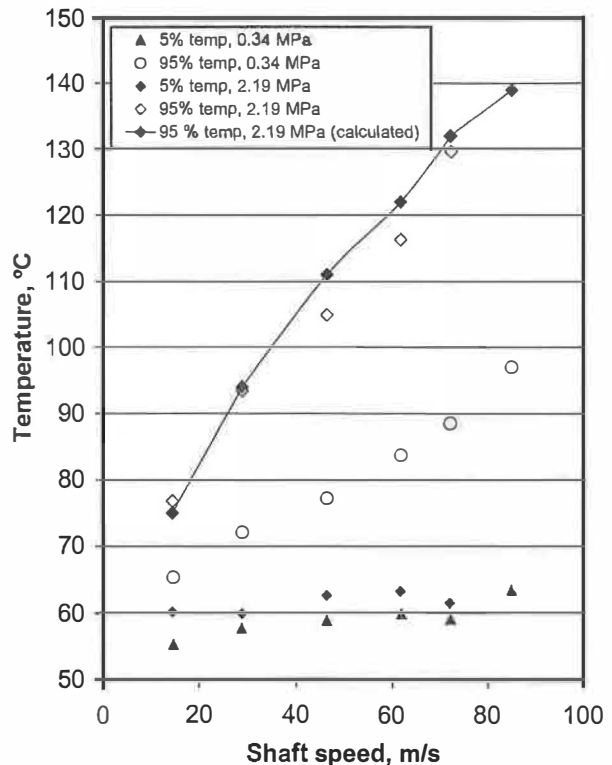


Fig. 9—Effect of shaft speed on second loaded pad temperatures—ISO VG 68 oil.

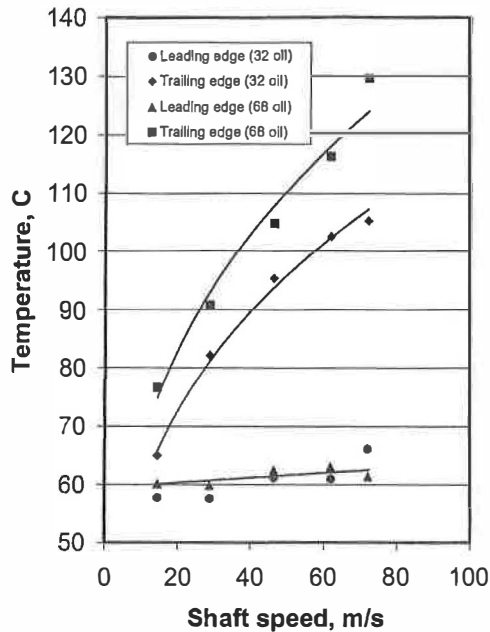


Fig. 10—Pad circumferential temperature rise as a function of shaft speed—2.19 MPa unit load.

respectively. In comparing the plots, the following observations were made:

- The ISO VG 68 oil resulted in significantly higher maximum bearing temperatures. For example, with a shaft speed of 72 m/s and a unit load of 2.19 MPa, the highest temperature recorded for ISO VG 68 was of the order of 130°C, compared to only 106°C for ISO VG 32.
- Both speed and load have a considerable effect on the increase in temperature from the leading to trailing edge. For example, with the ISO VG 68 oil and a unit load of 2.19 MPa, the increase at 72 m/s is of the order of 70°C (Fig. 10).
- Speed, load, and even oil viscosity have only a small effect on second loaded pad leading-edge temperature. For all of the test cases considered in this study, recorded leading-edge pad temperatures were of the order of 60° ± 5°C.

Figure 11 shows the effect of shaft speed, load, and oil viscosity on the second loaded pad 75% location temperature. Generally, all of these independent variables have a large influence on temperature at this location in much the same way as they do on maximum pad temperatures. It is noted that the 75% location temperatures are somewhat lower than the maximum pad temperatures with differences of as much as 20°C depending on load, speed, and oil type. Even so, the 75% location is an important indicator because babbitt integrity is also dependent on pressure, and the 75% location has a higher oil film pressure than the trailing edge of the pad.

Figures 12 and 13 show measured pad temperature profiles for a shaft speed of 72 m/s for the ISO VG 32 and 68 oils, respectively. In comparing these plots, the following observations were made:

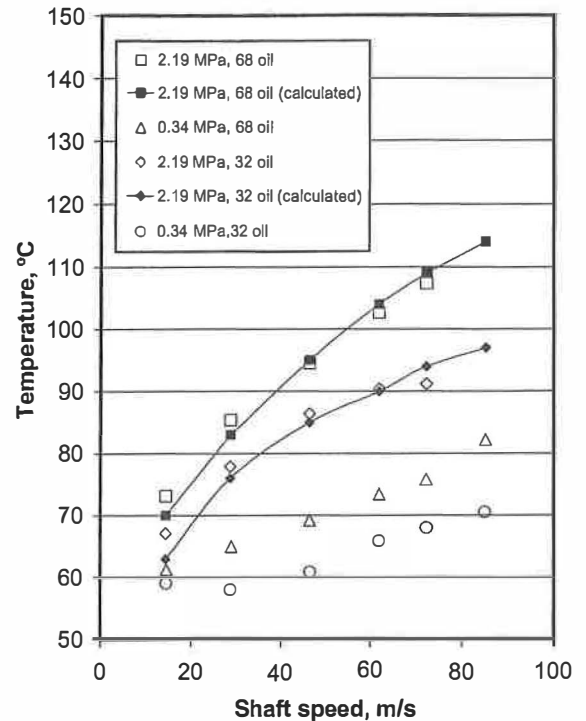


Fig. 11—75% pad location temperatures—second loaded pad.

- At higher loads, second loaded pad temperatures were significantly higher than the first loaded pad temperatures. This applied to both oils.
- Both loaded and unloaded pads had higher increases in pad temperature, leading to trailing edge, with the ISO VG 68 oil.

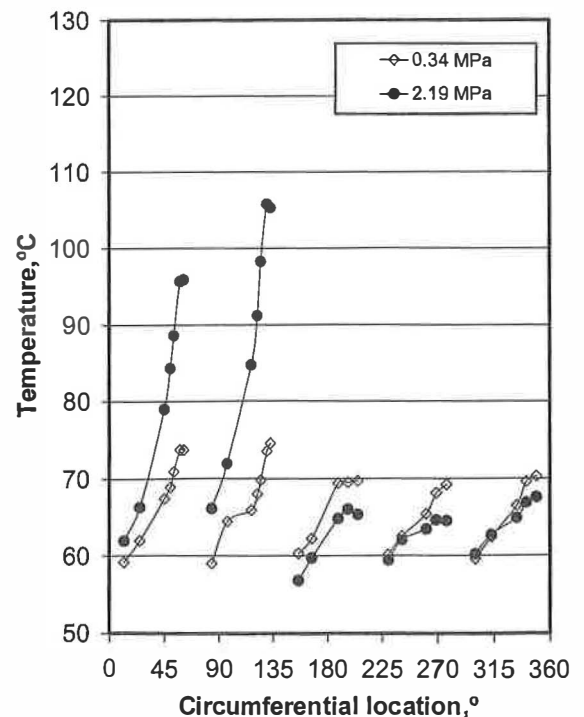


Fig. 12—Pad temperature profiles, 72 m/s—ISO VG 32 oil.

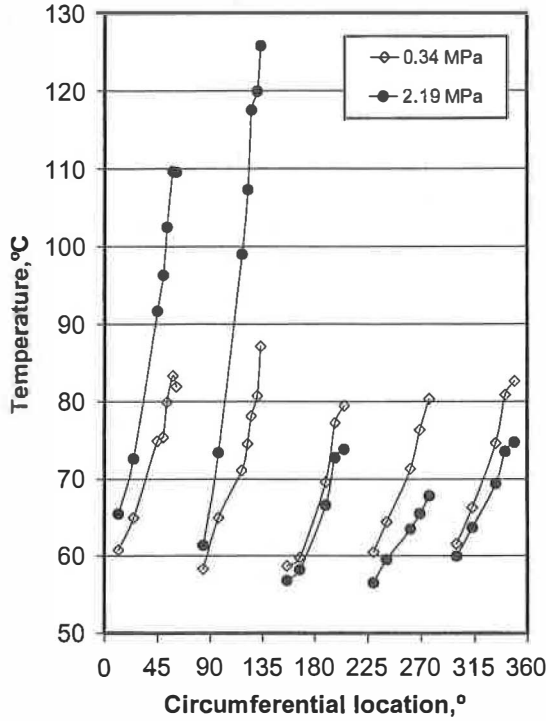


Fig. 13—Pad temperature profiles, 72 m/s—ISO VG 68 oil.

In the example shown in Fig. 13 at 2.19 MPa, the increase measured about 20°C on the unloaded pads, 45°C on the first loaded pad, and almost 70°C on the second loaded pad.

- Unlike the loaded pad temperatures, which rise with increasing load, unloaded pad temperatures fall with increasing load, which is more obvious with the thicker, ISO VG 68 oil.

There is good correlation between the experimental and calculated maximum and 75% location temperatures (Figs. 8, 9, and 11).

Bulk Oil Temperature Rise

Figure 14 shows the effect of load, speed, and oil viscosity on bulk oil temperature rise. Oil outlet temperatures are significantly higher in the case of the ISO VG 68 oil, which is attributed to the higher viscosity. Calculated and experimental results were in good agreement.

Bearing Displacements

Measurements showing eccentricities in PSJ bearings are rare. Tripp and Murphy (9) presented steady-state eccentricities for two five-pad PSJ bearings with 0.0 and 0.2 preloads.

Figure 15 shows shaft eccentricity as a function of Sommerfeld number for the two different oils tested in this study. The Sommerfeld numbers corresponding to the measured and theoretical data are based on the measured and calculated viscosity of the oil at the bearing outlet, respectively, and on the pad radial clearance:

$$S = \frac{P(C_p/R)^2}{UL\mu}$$

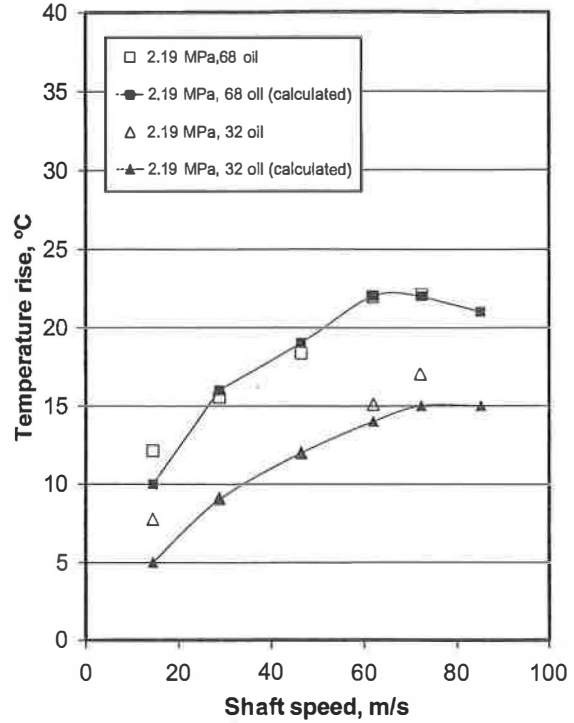


Fig. 14—Bulk oil temperature rise as a function of shaft speed.

where P is unit load, C_p is pad clearance, R is shaft radius, L is bearing width, U is shaft surface speed, and μ is oil viscosity.

The range of Sommerfeld numbers covered in Fig. 15 is based on a pad clearance-to-shaft ratio of 0.002, shaft speeds that ranged

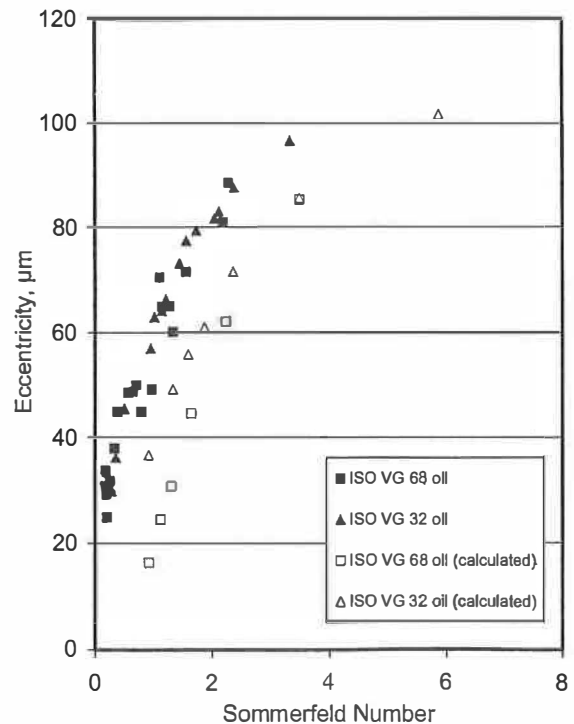


Fig. 15—Eccentricity measurements as a function of Sommerfeld number.

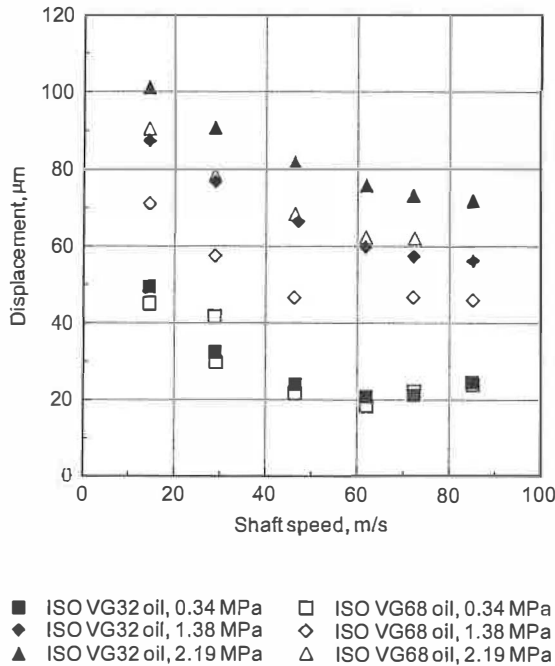


Fig. 16—Measured steady-state shaft vertical displacements.

between 14 and 85 m/s, and unit loads that ranged between 0.34 and 2.19 MPa. Bearing operating conditions such as these result in a range of Sommerfeld numbers that are typical of journal bearings in field applications. The higher Sommerfeld numbers represent highly loaded/low-shaft-speed operating conditions.

Comparison of calculated and measured eccentricity are only in fair agreement, which can be attributed to uncertainty in establishing the true zero position of the shaft. For these measured data, the zero position was based on 72 m/s and zero load operation. On the other hand, relative movement was very precisely measured by the instrumentation and methods described earlier, and comparison shows very good correlation between calculated and measured trends.

Measured steady-state shaft displacements for the two test oils are plotted in Fig. 16. The data represent the measured position of the shaft in the bearing clearance space for various operating conditions relative to the 72 m/s equilibrium position. The larger displacements represent a closer approach to the loaded pad surface; that is, a larger displacement indicates a smaller film thickness.

The maximum measured displacement was 100 μm . This occurred at 14 m/s with ISO VG 32 oil with a unit load of 2.19 MPa. At the same operating condition, the ISO VG 68 shaft displacement is 87 μm . For all data, the ISO VG 68 oil ran with 8–33% lower displacements, approximately 20% lower on average. The lower displacements are a measure of thicker oil films in the case of ISO VG 68 oil.

CONCLUSIONS

Tests have been performed on a 152-mm-diameter flood-lubricated 60% offset conventional PSJ bearing, comparing performance using ISO VG 32 and ISO VG 68 oils. Key conclusions arising from these tests are as follows:

- With the thicker ISO VG 68 oil, losses are larger than those recorded with the ISO VG 32 oil, but not significantly so. For example, at 72 m/s shaft speed, the difference in power loss was only of the order of 4 kW.
- The small difference in power loss is attributed to lower oil viscosity resulting from significantly higher loaded and unloaded pad temperatures measured in the case of ISO VG 68.
- Calculated losses and pad temperatures are in good agreement with the measured data. Calculations suggest that shear losses predominate (>80%), with churning losses making up most of the balance, and kinetic losses accounting for only 1–2% of the losses.
- In the case of the offset pivot bearing, loaded pad 75% location temperatures can be somewhat lower than maximum pad temperatures, which occur close to the pad's trailing edge.
- Speed, load, and oil viscosity had only a small effect on the leading-edge temperature of the second loaded pad.
- Calculated and measured eccentricity trends correlate well. Comparison of calculated and measured eccentricity are only in fair agreement, which is attributed to uncertainty in establishing the true zero position of the shaft.
- The ISO VG 68 tests ran with lower eccentricities, representing thicker oil films. This is at the expense of higher bearing temperatures and power losses.

CLOSURE

Some assessment can be made using Figs. 11 and 16 when considering a change in oil viscosity grade. The data indicate that a switch from ISO VG 68 to ISO VG 32 in a comparable bearing will give a substantial decrease in pad temperature for surface speeds above 45 m/s. Eccentricity is already low at the higher speeds, and a 20% increase using a lighter oil does not impose any serious consequence. Conversely, changing to an ISO VG 68 oil at higher speeds may result in unacceptably high pad temperatures, depending on the magnitude of the load.

Pad temperatures for both oils are low at the lower speeds. Here, a change to ISO VG 68 can be used to increase film thickness with only a small increase in pad temperature and power loss. It is not desirable to switch to ISO VG 32 at the lower speeds because of the high eccentricities (thin oil films), unless the load is substantially lower than 2.19 MPa.

ACKNOWLEDGMENTS

The authors are grateful to Kingsbury, Inc., and the National Research Council of Canada for permission to publish the results of this study. The authors particularly want to thank Brian Liko and Tim Breithaupt of the National Research Council of Canada, without whose efforts this work would not have been possible.

REFERENCES

- (1) Brockwell, K., DeCamillo, S. and Dmochowski, W. (2001), "Measured Temperature Characteristics of 152 mm Diameter Pivoted Shoe Journal Bearings with Flooded Lubrication," *Tribol. Trans.*, **44**, pp 543–550.
- (2) Brockwell, K., Dmochowski, W. and DeCamillo, S. (2002), "Effect of Oil Flowrate on the Steady-State Performance of Pivoted Shoe Journal Bearings," *Tribol. Trans.*, submitted for publication.

- (3) Simmons, J. and Dixon, S. (1994), "Effect of Load Direction, Preload, Clearance Ratio, and Oil Flow on the Performance of a 200 mm Journal Pad Bearing," *Tribol. Trans.*, **37**, pp 227-236.
- (4) Simmons, J. and Lawrence, C. (1996), "Performance Experiments with a 200 mm, Offset Pivot Journal Pad Bearing," *Tribol. Trans.*, **39**, pp 969-973.
- (5) DeChoudhury, P. and Masters, D. (1983), "Performance Tests of Five-Shoe Tilting-Pad Journal Bearing," *Tribol. Trans.*, **27**, pp 61-66.
- (6) DeChoudhury, P. and Barth, E. (1981), "A Comparison of Film Temperatures and Oil Discharge Temperature for a Tilting-Pad Journal Bearing," *ASME J. Lubr. Technol.*, **103**, pp 115-119.
- (7) Brockwell, K. and Kleinbub, D. (1989), "Measurements of the Steady State Operating Characteristics of the Five Shoe Tilting Pad Journal Bearing," *Tribol. Trans.*, **32**, pp 267-275.
- (8) Pettinato, B. and DeChoudhury, P. (1999), "Test Results of Key and Spherical Pivot Five-Shoe Tilt Pad Journal Bearings—Part I: Performance Measurements," *Tribol. Trans.*, **42**, pp 541-547.
- (9) Tripp, H. and Murphy, B. (1984), "Eccentricity Measurements on a Tilting-Pad Bearing," *ASME Trans.*, **28**, pp 217-224.
- (10) Dmochowski, W., Brockwell, K., DeCamillo, S. and Mikula, A. (1992), "A Study of the Thermal Characteristics of the Leading Edge Groove and Conventional Tilting Pad Bearings," *ASME J. Tribol.*, **115**, pp 219-226.
- (11) API Standard 670 (1986), "Vibration, Axial-Position, and Bearing Temperature Monitoring Systems," American Petroleum Institute, Washington, DC.
- (12) Dorfman, L. (1963), *Hydrodynamic Resistance and the Heat Loss of Rotating Solids*, Oliver and Boyd, Edinburgh, London.

APPENDIX A

Churning Losses

For disk, under turbulent regime:

$$M = C_M \delta \omega^2 r^5$$

(Dorfman (12)) where C_M = moment coefficient, δ = oil density, ω = angular speed of the disk, r = radius of the disk, and M = friction torque.

But

$$C_M = 0.982(\log \text{Re})^{-2.58}$$

(Dorfman (12)) where $\text{Re} = \text{Reynolds number} = r2\omega/\nu$ and $\nu = \text{kinematic viscosity}$.

For disk, power loss:

$$P_D = M\omega = C_M \delta \omega^3 r^5 / 4$$

For cylinder, power loss:

$$P_C = 4LP_D/r = LC_M \delta \omega^3 r^4$$

For part of a cylinder, power loss:

$$P_{CH} = P_C(2\pi - n\varphi)r/2\pi r$$

where n = number of pads and φ = angular extent of pads.

Hence,

$$P_{CH} = 0.982(1 - (n\varphi/2\pi)) \times L \delta \omega^3 r^4 \times (\log \text{Re})^{-2.58}$$

Kinetic Losses

Kinetic energy:

$$E_K = mV^2/2$$

but $m = \delta Q$ and $V = \omega r/2$.

Therefore,

$$E_K = \delta Q \omega^2 r^2 / 8$$

where δ = oil density, Q = oil flow rate, ω = angular speed of the disk, and r = radius of the shaft.

